Accepted Manuscript

Characterization and disintegrability under composting conditions of PLA-based nanocomposite films with thymol and silver nanoparticles

Marina Ramos, Elena Fortunati, Mercedes Peltzer, Alfonso Jimenez, José María Kenny, María Carmen Garrigós

PII: S0141-3910(16)30145-8

DOI: 10.1016/j.polymdegradstab.2016.05.015

Reference: PDST 7962

To appear in: *Polymer Degradation and Stability*

Received Date: 30 December 2015

Revised Date: 2 May 2016

Accepted Date: 16 May 2016

Please cite this article as: Ramos M, Fortunati E, Peltzer M, Jimenez A, Kenny JM, Garrigós MC, Characterization and disintegrability under composting conditions of PLA-based nanocomposite films with thymol and silver nanoparticles, *Polymer Degradation and Stability* (2016), doi: 10.1016/j.polymdegradstab.2016.05.015.

Characterization and disintegrability under composting conditions of PLA-based nanocomposite films with thymol and silver nanoparticles

Marina Ramos[1*], Elena Fortunati[2], Mercedes Peltzer[3,4], Alfonso Jimenez[1], José María Kenny[2,5], María Carmen Garrigós[1]

1. Dept. Analytical Chemistry, Nutrition & Food Sciences, University of Alicante, Campus de San Vicente del Raspeig S/N, 03690, Alicante, Spain

2. Materials Engineering Center, UdR INSTM, University of Perugia, Strada Pentima Bassa 4, 05100 Terni, Italy

3. Laboratory of Obtention, Modification, Characterization and Evaluation of Materials (LOMCEM). Department of Science and Technology, University of Quilmes, Av. Rivadavia 2358, 6.º D, C1034ACP, Bernal, Argentina.

4. National Scientific and Technical Research Council (CONICET), Av. Rivadavia 1917, C1033AAJ, Ciudad autónoma de Buenos Aires, Argentina

5. Institute of Polymer Science and Technology, CSIC, Calle Juan De La Cierva, 3, 28028 Madrid, Spain

*All correspondence should be addressed to this author. Tel: +34 965903400. Ext 3117

Fax: +34 965903697. E-mail: marina.ramos@ua.es

ABSTRACT

Active nanocomposite films based on poly(lactic acid) (PLA), thymol and silver nanoparticles (Ag-NPs) were prepared and characterised. PLA films containing 6 and 8 wt% thymol and 1 wt% Ag-NPs were processed by extrusion to obtain binary and ternary formulations. The addition of thymol and Ag-NPs modified the PLA thermal, optical and barrier properties; in particular water vapour permeability (WVP), maintaining oxygen transmission rate (OTR) values unchanged. Homogeneous surfaces in all films were obtained as proved by FESEM micrographs. The presence of the active additives enhanced the disintegration rate of PLA under composting conditions, which was completed in 14 days. Results suggest that these nanocomposite films could be considered promising degradable active packaging materials with low environmental impact.

KEYWORDS: poly(lactic acid); thymol; silver nanoparticles; active packaging; disintegration; characterization.

1. Introduction

The preservation of the environment and the atmospheric and soil pollution caused by fossil fuel-derived plastics have focused on rising research interest towards the development of bio-based and biodegradable materials in high-impact sectors, such as food packaging [1]. These materials are under development by strictly following the guidelines for the efficient use of natural and renewable resources, keeping the properties of conventional thermoplastics to preserve food quality and consumer safety, while reducing waste disposal and CO_2 footprint by offering new recycling and recovery options [2]. Among them, poly(lactic acid) (PLA) has received attention mostly due to its inherent renewable source, adequate optical and mechanical properties, and high biodegradation/biocompatibility capabilities to be easily degraded into water and CO_2 [3]. In addition, PLA is classified as "Generally Recognized as Safe" (GRAS) for food packaging applications, fulfilling the requirements to be in direct contact with aqueous, acidic and fatty foods [4].

Innovations in food packaging have focused on the development of active nanocomposites, which are particularly useful in emerging technologies due to their improved structural integrity and barrier properties obtained by the addition of nanomaterials (either nanoclays or metal nanoparticles), and the increase in antimicrobial/antioxidant properties in most cases by the action of active additives and/or the own nanofiller. The use of nanofillers in innovative food packaging materials has also resulted in improving some of their key properties, such as strength and flexibility, barrier to gases, moisture stability and higher resistance to heat and cold [2, 5-7]. Nanocomposites with metal nanoparticles are gaining importance in active packaging, since they could play a double role, as nanofillers (enhancing mechanical and barrier properties) and active agents with antimicrobial performance [8-11]. In this

context, silver nanoparticles (Ag-NPs) have been studied by their strong antimicrobial effect to a wide range of microorganisms in health, food packaging and textile industries besides of a number of environmental applications. Ag-NPs have been already used in some commercial products by their antimicrobial performance and they have been approved by the US Food and Drug Administration (FDA), US Environmental Protection Agency (EPA), Society of Industrial-Technology for Antimicrobial Articles (SIAA) of Japan, Korea's Testing and Research Institute for Chemical Industry and Functional Textile & Clothing Testing Institute (FITI) in Korea [12]. Ag-NPs have been also used in polymer formulations by their stability at high temperatures and low volatility to improve the antimicrobial resistance of polymers used in specific applications, such as food packaging [13-16]. According to the Council Directive 94/36/EC (1994), silver is accepted as food additive with the code E174 if used as "external coating of confectionary, decoration of chocolates, liqueurs". Nevertheless, in food contact materials, Ag-NPs are not still allowed, but the presence of certain silver zeolites is already authorized in plastic food containers and rubber seals [17]. Therefore, toxicological issues should be taken into account in all new developed materials with Ag-NPs in their composition. Lavorgna et al. synthesized active nanocomposites by loading chitosan with Ag-MMT nanoparticles. The successful intercalation and the interaction between chitosan and Ag-NPs led to the enhancement of the thermal stability of the developed active nanocomposites [18].

The combination of additives from natural sources with antimicrobial and/or antioxidant performance with nanofillers to improve polymer characteristics while having positive impact on food shelf-life extension and safety has been also introduced in this novel concept of active nanocomposites [19]. In particular, thymol has been extensively used as a natural active antimicrobial and antioxidant agent. Different strategies for the

incorporation of this type of active agents to packaging materials have been proposed, by the inherent volatility of these compounds, resulting in some drawbacks related to their thermal stability and full control of the release kinetics [20-21]. Recent studies have proposed the use of new methodologies to improve the permanence of active agents during polymer processing. One interesting approach consists of controlling the addition times of the nanocomposite components at the melting state. Other possibility to protect volatile essential oils during processing is based on reinforcement with nanofillers [20, 22-24] or encapsulation techniques [25-28]. Thymol is recognized by the Food and Drug Administration (FDA) as a GRAS substance for its use in direct contact with food [29]. It is used in active packaging by its high diffusion rate into most of the polymer matrices and its ability to be released, minimizing the bacterial growth and delaying the oxidation processes in food [21].

In a previous study, the influence of thymol and Ag-NPs on the degradation of PLA-based nanocomposites under composting conditions in dog-bone tensile bars was reported. These formulations were used for the analysis of thermal, morphological, and mechanical properties of these PLA-based nanocomposites, which showed suitable properties to be used as biodegradable active food packaging systems, with clear improvement in the inherent biodegradable character of PLA after the addition of both additives [23].

Nano- and thin-film technologies based on novel systems associating metal particles and natural additives to polymer matrices open a broad range of new applications, such as bio-films with antimicrobial effect for the food industry. In this context, the present work aims to develop biodegradable thin nanocomposite films (around 40 μm thick) based on PLA with thymol and Ag-NPs as active additives to extend their applicability

to packaging systems [30]. For this purpose, the evaluation of their thermal, morphological, optical, barrier and disintegration properties is presented in this work.

2. Materials and methods

2.1. Materials

Thymol (99.5 % purity) was supplied by Sigma-Aldrich (Madrid, Spain). Commercial silver nanoparticles (Ag-NPs), P203, with a size distribution range of 20-80 nm, were purchased from Cima Nano-Tech (Saint Paul, MN, USA). Ag-NPs were thermally treated at 700 ºC for 1 h as reported elsewhere [31]. A commercial poly(lactic acid) PLA-4060D (T_g = 58 ºC, 11-13 wt% D-isomer) was supplied in pellets by NatureWorks Co., (Minnetonka, MN, USA).

2.2. Nanocomposite films preparation

PLA-based nanocomposites were processed in a twin-screw microextruder (Dsm Explore 5&15 CC Micro Compounder, Heerlen, The Netherlands). PLA pellets were dried overnight at 45 ºC before extrusion to prevent polymer hydrolysis during processing. A 170-180-190 ºC temperature profile and a screw speed of 150 rpm were used in the extrusion process. Different binary and ternary PLA-based formulations were obtained (Table 1): three binary systems, containing 6 and 8 wt% of thymol (PLA/T6 and PLA/T8, respectively) or 1 wt% of Ag-NPs (PLA/Ag); and two ternary systems, containing 6 wt% of thymol and 1 wt% of Ag-NPs (PLA/Ag/T6), and 8 wt% of thymol and 1 wt% of Ag-NPs (PLA/Ag/T8). An additional sample without any additive was also prepared as control (PLA).

For binary systems, a total mixing time of 6 min was used. Thymol was added in the last 3 minutes and the screw speed was then reduced to 100 rpm to limit losses by

vaporization. For ternary systems (PLA/Ag/T6, PLA/Ag/T8), a masterbatch of PLA and Ag-NPs was first processed in the extruder during 3 min and it was then combined with 6 or 8 wt% of thymol for 3 additional minutes. After mixing, PLA and PLA nanocomposite films were obtained in a hot-press with a head force of 1500 N and a maximum temperature of 195 ºC (Table 1); Films thickness was determined to be around 40 μm with a 293 MDC-Lite Digimatic Micrometer (Mitutoyo, Japan) at five random positions.

2.3. Characterization of nanocomposite films

PLA-based nanocomposite films were characterized in terms of their thermal, morphological, optical (colour, light transmission), and barrier (oxygen transmission rate, water vapour permeability) properties.

2.3.1. Thermal properties

Thermogravimetric analysis (TGA) was carried out by using a TGA Seiko Exstar 6300 (USA) instrument. Samples (7 mg) were heated from 25 to 700 ºC at 10 ºC min^{-1} heating rate under nitrogen atmosphere (flow rate 50 mL min^{-1}). Analyses were performed in triplicate.

Differential scanning calorimetry (DSC) measurements were conducted, in triplicate, by using a DSC Mettler Toledo 822/e (Schwerzenbach, Switzerland) under nitrogen atmosphere (50 mL min^{-1}). Samples (3 mg) were introduced in aluminium pans (40 μL) and were submitted to the following thermal program: -25 to 200 ºC at 10 ºC min^{-1}, with two heating and one cooling scans. Glass transition temperature (T_g) was determined in the second heating scan.

2.3.2. Field emission scanning electron microscopy (FESEM)

The surface profiles of neat PLA and PLA active nanocomposite films were evaluated by FESEM (Supra 25-Zeiss, Jena, Germany) to study their homogeneity and the influence of thymol and Ag-NPs on the polymer morphology. Samples were coated with a gold layer prior to analysis in order to increase their electrical conductivity by using a B7341 Agar automatic sputter coater (Agar Scientific Ltd, Stansted, United Kingdom).

2.3.3. Optical properties

The light transmission of PLA-based films was determined, in triplicate, by using a Perkin Elmer Lambda 35 UV–Vis spectrophotometer (Waltham, MA, USA). Tests were carried out at 500 nm in transmittance (%) mode to evaluate the transparency of all films in the visible region. Each film was cut in 2.5 x 2.5 cm^2 strips.

Modifications on the films colour caused by additives were determined with a Konica CM-3600d COLORFLEX-DIFF2 colorimeter (Reston, VA, USA) using the CIELab colour parameters. Changes in L^* (lightness), a^* (red-green coordinate) and b^* (yellow-blue coordinate) were determined from the results obtained with the colorimeter. The instrument was calibrated with a white standard tile. Measurements were taken at five different random locations over the film surface and average values were calculated. Total colour differences (ΔE^*) were calculated by using Eq. (1), comparing with a neat PLA film (standard):

$$\Delta E^* = [(\Delta L^*)^2+(\Delta a^*)^2+(\Delta b^*)^2]^{1/2} \quad (1)$$

where $\Delta L^* = L^*_{standard} - L^*_{sample}$, $\Delta a^* = a^*_{standard} - a^*_{sample}$ and $\Delta b^* = b^*_{standard} - b^*_{sample}$.

2.3.4. Barrier properties

Oxygen transmission rate (OTR) is defined as the total amount of oxygen passing through a plastic film per time unit. An oxygen permeation analyser (8500 model Systech, Metrotec S.A, Spain) was used for OTR tests with pure oxygen (99.9 %). Film samples were cut into 14-cm diameter circles and they were clamped in the diffusion chamber at 25 ºC before testing. Tests were performed in triplicate and average values were expressed as oxygen transmission rate per film thickness (OTR*e).

Water vapour permeability (WVP) was determined gravimetrically by following the ASTM E 96M-05 Standard test method. Films were cut in circles of 95 mm diameter and mounted on stainless steel permeation cells containing anhydrous calcium chloride, sealed with paraffin. These cells were placed in a climatic chamber (Dycometal, Barcelona, Spain) at 23 ºC and 50% relative humidity (RH). The amount of water vapour transferred through the film and absorbed by the desiccant was determined from the weight gain of the cell after 24 h. A minimum of seven determinations were taken to plot the weight variation with time resulting in a linear characteristic graph. Water vapour transmission (WVT) was calculated with Eq. (2).

$$WVT = (G/t)/A \qquad (g \cdot h^{-1} \cdot m^{-2}) \qquad (2)$$

where A is the film area exposed (0.005 m^2) and G/t is the slope obtained from plotting the weight gained in the permeation cell (G, grams) versus time (t, hours).

The water vapour permeability (WVP) of films was determined, in triplicate, by using Eq. (3).

$$WVP\ (kg \cdot m \cdot Pa^{-1} \cdot s^{-1} \cdot m^{-2}) = WVT \times e / (S(R_1 - R_2)) \qquad (3)$$

where *e* is the film thickness, S is the saturation vapour pressure at 23 ºC, and (R_1-R_2) is the difference in relative humidity between the exterior and interior of the permeation cell (0.5).

2.4. Disintegrability under composting conditions

Disintegration tests under composting conditions were performed by following the ISO 20200 standard method. A commercial compost with fixed amounts of sawdust, rabbit food, starch, sugar, oil and urea was used. Aerobic conditions were guaranteed by mixing the compost softly and by the periodical addition of water according to the standard requirements. Testing samples (20 x 20 mm^2 films), in triplicate, were weighted and buried at 5 cm depth in perforated boxes containing the prepared mix and were incubated at 58 ºC.

Several disintegration times were selected to recover samples from burial: 0, 1, 2, 4, 7 and 14 days. Samples were washed immediately after collection with distilled water to remove traces of compost extracted from the container and were further dried at 37 °C for 24 h before gravimetrical analysis. The disintegrability value for each material at different times was obtained by normalizing the sample weight with the value obtained at the initial time. Photographs of recovered samples were also taken for visual evaluation.

2.5. Statistical analysis

Statistical analysis of results was performed with SPSS commercial software (Version 15.0, Chicago, IL). A one-way analysis of variance (ANOVA) was carried out. Differences between means were assessed on the basis of confidence intervals using the Tukey test at a $p < 0.05$ significance level.

3. Results and discussion

3.1. Thermal properties

The effect of the addition of thymol and Ag-NPs on the thermal properties of PLA-based films was investigated by DSC and the main results are summarized in Table 2, while the thermograms obtained for the second heating scan are shown in Fig. 1a. The glass transition temperature (T_g) of PLA and all nanocomposites was clearly observed, due to the amorphous character of the PLA used in this study, while no crystallization or melting phenomena were detected (Fig. 1a).

The addition of Ag-NPs to PLA (PLA/Ag) did not reveal significant differences with respect to neat PLA in terms of T_g ($p > 0.05$), in agreement with previous studies [16, 23]. However, thymol-based binary and ternary systems showed a significant decrease ($p < 0.05$) in T_g values with differences higher than 10 °C (Table 2). This reduction in T_g by the addition of thymol was related with the higher mobility of the polymer macromolecules caused by the increase in the free volume of the matrix, promoting the torsion oscillation of the carbon backbone due to a plasticizing effect of thymol. It is well known that the addition of low molecular weight compounds decreases the PLA rigidity and brittleness by reducing its glass transition temperature and increasing the mobility of macromolecules [32-33]. A similar T_g shift to lower temperatures by the incorporation of thymol to different polymer matrices producing a plasticization effect was also reported in a previous work [20]. A significant decrease in T_g caused by the incorporation of thymol to PLA-based films was also reported by other authors [22, 34]. A similar behaviour was reported for α-tocopherol, resveratrol, buthylated hydroxytoluene (BHT) and tert-butylhydroquinone added to PLA [33, 35-36]. In all cases, an effective plasticizing effect was observed and it was related to the addition of these compounds, with the consequent decrease in T_g.

The thermal stability of neat PLA and PLA active nanocomposite films was studied with TGA under nitrogen atmosphere. Fig. 1b and Fig. 1c show the weight loss (TG)

and derivative curves (DTG) of the obtained PLA-based films. A main degradation peak around 332-363 ºC associated to PLA thermal degradation was observed in all materials. A first degradation step starting at around 120 ºC was also detected, and it could be related to the thymol degradation. This fact confirms the permanence of a detectable amount of thymol in the nanocomposites after processing at high temperatures, as already reported in a previous work [23]. Moreover, the remaining amount of the active additive in the polymer matrix after processing was estimated from the obtained TG curves. For binary systems, PLA/T8 and PLA/T6, 5.63 ± 0.02 wt% and 4.2 ± 0.2 wt%, respectively, were obtained; and for ternary systems, PLA/Ag/T8 and PLA/Ag/T6, the concentrations of remaining thymol after processing were 6.0 ± 0.2 wt% and 4.2 ± 0.2 wt%, respectively. These results revealed significant differences ($p < 0.05$) between binary and ternary systems with 8 wt% of thymol. The main TGA parameters, i.e the initial degradation temperature (T_{ini}) determined at 5 % weight loss and the maximum degradation temperature (T_{max}) for the main peak (associated to the PLA thermal degradation), are shown in Table 2. The separate addition of thymol and Ag-NPs into PLA matrices did not affect significantly the thermal behaviour of the polymer matrix in terms of T_{max} and T_{ini} ($p > 0.05$). However, a significant reduction ($p < 0.05$) was observed for PLA-based active nanocomposites with thymol and Ag-NPs, suggesting some loss in the PLA thermal stability. This phenomenon could be related with some degradation of these materials during processing caused by the presence of metal nanoparticles, which enhanced the thermal conductivity of the nanocomposites, speeding up the degradation process of the polymeric matrix [37].

Table 2

Figure 1

3.2. Morphological analysis

The surface morphology and microstructure of PLA and active nanocomposite films were studied by FESEM in order to evaluate the influence of the incorporation of thymol and Ag-NPs into the polymer matrix. Fig. 2 shows the FESEM surface micrographs obtained for neat PLA and PLA nanocomposites after processing. Homogeneous and smooth surface morphologies were observed for all materials, with no apparent effect of the addition of thymol and Ag-NPs into the PLA matrix. Similar morphologies were observed by other authors for PLA and other polymer matrices blended with Ag-NPs or thymol [16, 38-40]. Rhim et al. reported also smooth surfaces with evenly dispersed silver nanoparticles on the PLA film surface [40]. These results demonstrate a positive combination between PLA, thymol and Ag-NPs to obtain homogeneous surfaces after film processing.

Figure 2

3.3. Optical properties

All PLA-based films were visually homogeneous and transparent regardless of their composition (Fig. 3). The colour distribution observed in all films suggests that additives were uniformly distributed through the polymer matrix during processing. However, nanocomposite films containing Ag-NPs showed some darkening in the initially clear surface as well as some decrease in transparency, which is an important physical property in food packaging films where clarity is desirable [41]. In fact, it has been reported that the incorporation of some additives to PLA can lead to substantial modifications and transparency losses, representing an important drawback for consumer acceptance [42]. Rhim et al. suggested that surface plasmon phenomena

caused by silver nanoparticles and phenolic compounds, such as thymol, may modify PLA colour during processing and storage leading to some darkening of films [40].

Figure 3

Results obtained for colour and transmittance at 500 nm of all films are shown in Table 3. The modifications in surface colour in the PLA binary and ternary films was significant ($p < 0.05$) depending on the additive. While some decrease ($p < 0.05$) in film lightness (L-value) was observed in PLA films containing Ag-NPs, it slightly increased in those with thymol ($p < 0.05$) when compared to values obtained for the neat PLA film. In addition, a^* and b^* parameters were modified by the presence of both additives (Table 3). In particular, Ag-NPs-containing binary and ternary systems resulted in significant shifts ($p < 0.05$) in a^* and b^* towards positive values, indicating an increasing trend in redness and yellowness, respectively, of the active nanocomposite films. Consequently, the total colour difference, ΔE^*, of those films with Ag-NPs increased significantly ($p < 0.05$) compared to neat PLA. This behaviour can be explained by the development of brown colour in nanocomposite films caused by the plasmonic effect of Ag-NPs [43]. Regarding binary systems containing thymol, the obtained results indicated that these films were not much different in colour compared to neat PLA.

PLA is a transparent polymer with a transmittance close to 95% in the visible region (Table 3), as already reported [41]. The evaluation of the light transmission of PLA-based nanocomposites at 500 nm revealed that all the binary and ternary films were, in general, highly transparent, showing transmittance values higher than 90 %. A slight decrease ($p < 0.05$) in transmittance was observed in binary systems containing thymol, which might be due to the colourless transparent appearance of this additive. The

inclusion of Ag-NPs into the PLA films also produced some significant reduction ($p < 0.05$) in transparency, which was related to the prevention of light transmission by the nanoparticles homogeneously dispersed through the polymer matrix [14]. The obtained results suggested that the amount of additives, thymol and Ag-NPs, used in these formulations did not affect dramatically the colour and transparency of PLA films. Therefore, their incorporation into the PLA matrix could be suitable for food packaging applications without compromising, to an unacceptable degree, its optical properties.

Table 3

3.4. Barrier properties

The effect of the addition of thymol and Ag-NPs on the barrier properties (OTR and WVP) of PLA-based films was studied and the main results are shown in Table 2. Films with low oxygen permeability are desirable for food preservation, since oxygen can accelerate food oxidative degradation and facilitate the growth of aerobic microorganisms, thereby shortening the food shelf-life [11]. The *OTR·e* values obtained in this study showed that the oxygen barrier offered by neat PLA was not significantly modified ($p > 0.05$) in the presence of additives at the studied concentrations.

The evaluation of the barrier properties to water vapour of these PLA-based nanocomposite films is important to assess their possibilities to be used as food packaging materials since one of their main functions should be to decrease the moisture transfer between food and the surrounding environment keeping quality and increasing shelf-life [44]. Water vapour barrier in films could be considered as the balance between the hydrophobic/hydrophilic characteristics of all their components. The WVP of the neat PLA film (Table 2) was not significantly affected ($p > 0.05$) by the incorporation of Ag-NPs (PLA/Ag). This behaviour may be due to the spherical

shape of silver particles and their high dispersion in the polymer matrix which may not develop a tortuous pathway to limit water vapour diffusion [43].

It has been stated that high water vapour permeabilities of films intended for food packaging could restrict considerably their use [45]. In this case, the addition of thymol to PLA-based films resulted in a significant decrease ($p < 0.05$) in WVP values for binary and ternary systems, up to 40 % compared to those values obtained for the neat PLA film. These results could be explained by the repulsion to water molecules caused by the addition of a highly hydrophobic component, such as thymol, at high concentrations [46]. Therefore, these thymol-containing nanocomposites allowed an important improvement in barrier properties to water vapour, which is a remarkable feature in food packaging applications, especially at storage conditions with high RH. Similar results were found by other authors under equivalent environmental conditions (23 ºC, 45% RH), reporting a WVP value of 1.99×10^{-14} kg m m^{-2} s^{-1} Pa^{-1} for neat PLA, and a 25 % reduction in WVP for PLA films loaded with α-tocopherol (4 wt%) [33]. Meanwhile, the addition of 2 wt% marigold flower extract containing astaxanthin resulted in the decrease in 21 % in WVP of PLA, which was attributed to the hydrophobic nature of this extract [47]. Conversely, no significant differences were observed for WVP of PLA/PCL-based films with thymol (3-12 wt %) compared to PLA/PCL films, showing 2.54×10^{-14} kg m m^{-2} s^{-1} Pa^{-1} as WVP value [22, 34].

3.5. Disintegrability under composting conditions

Biodegradability tests are necessary to evaluate the environmental impact of plastic materials and to find solutions to avoid the disturbing accumulation of polymers after their commercial shelf-life. The disintegrability of PLA and PLA active nanocomposite films under composting conditions was studied to evaluate their degradation in natural

environments. The visual evaluation of all samples at different degradation times showed considerable changes, with a clear whitening, loss of transparency and evident deformation and size reduction after 2 days (Fig. 4). These results were indicative of the beginning of the hydrolytic degradation as it was reported in a previous study [23]. The hydrolytic degradation process in PLA nanocomposites and the increase in their opacity can be attributed to various simultaneous phenomena, such as the formation of low molar-mass degradation by-products during hydrolysis due to the water absorption and the increase in PLA crystallinity [48]. After 4 days, neat PLA and binary and ternary systems became brittle and just small pieces of films were recovered. The faster degradation of these active nanocomposite films when compared to previous results obtained with injection moulded samples [20] can be explained by the lower thickness of films, which showed considerable modifications in colour and a general loss of transparency after 7 days under composting conditions.

Figure 4

Fig. 5 shows the evolution of disintegrability values (%) of films with time. A progressive degradation of samples with the burial time was obtained, which was visually corroborated by the clear whitening and transparency loss and evident deformation observed in samples (Fig. 4). A similar behaviour was reported by Fortunati et al., who indicated that the PLA hydrolysis begins in the amorphous region of the polymer structure producing an overall increase in polymer crystallinity [16]. This increase in crystallinity was expectable by the intrinsic amorphous character of the PLA used in this work with a large content in D-LA enantiomer [49]. Furthermore, results obtained before the beginning of the burial test (day 0) suggested that the influence of thymol on PLA degradation profile is important, since significantly higher

disintegration values were obtained for PLA/T6, PLA/T8, PLA/Ag/T6 and PLA/Ag/T8 compared to PLA or PLA/Ag samples ($p < 0.05$). It was described that thymol hydroxyl groups can contribute to PLA hydrolysis after absorbing water from the composting medium, resulting in a noticeable increase in disintegrability values for thymol-containing PLA nanocomposites [23].

After 4 days of treatment, no significant differences ($p > 0.05$) were observed for all samples regardless of their composition and the burial time (Fig. 5), showing similar weight loss and disintegrability ratio. It should be also highlighted that the testing temperature (58 °C) was higher than the T_g of the PLA-based films, previously reported in the 40-45 °C range, resulting in some induction of the crystallization process into the amorphous zones in the polymer matrix and chain mobility, accelerating the hydrolytic degradation process. This behaviour could also be related to the low thickness of the tested samples [50].

It was observed that after 14 days of the burial test all materials reached complete degradation with weight losses higher than 90% (as indicated in the ISO 20200 standard for a biodegradable material). These results suggest that these active nanocomposite films could be used as biodegradable materials requiring short disintegration times.

Figure 5

4. Conclusions

Degradable active films based on PLA, thymol and Ag-NPs were successfully obtained by extrusion and further characterized in their main thermal, morphological, optical and barrier properties. Disintegrability under composting conditions was also studied. It was found that the presence of thymol and Ag-NPs through the PLA matrix influences the thermal stability of the ternary systems. The addition of thymol to PLA-based films

resulted in a decrease in T_g of PLA, due to a slight plasticizing effect of this additive. Optical properties suggest that the amount of additives, thymol and Ag-NPs, used in these formulations did not affect dramatically the colour and transparency of PLA films. FESEM micrographs showed a good incorporation of both additives and homogeneous film surfaces. An enhancement in the barrier properties to water vapour was also obtained by the incorporation of thymol, which provides improved protection to packaged food. Additionally, the degradation study of active nanocomposite films under composting conditions showed that the inherent degradable character of PLA remained after the incorporation of these additives. In fact, the incorporation of 8 wt% of thymol to PLA-based formulations increased the disintegration rate of the polymer matrix, due to the presence of the reactive free hydroxyl groups in the thymol molecule. The combination of thymol and Ag-NPs induced higher degradation rates, suggesting their advantages in industrial applications where degradation could be an issue, such as in food packaging.

Further work is currently on-going to evaluate the multifunctional applicability of the proposed active nanocomposite films, such as antioxidant and antibacterial behaviour or kinetics release from the polymer matrix, to ensure their ability to be used in food packaging applications.

Acknowledgements

Authors would like to thank Spanish Ministry of Economy and Competitiveness for financial support (MAT-2015-59242-C2-2-R). Marina Ramos would like to thank University of Alicante (Spain) for UAFPU2011-48539721S pre-doctoral research grant.

References

[1] Alix S, Mahieu A, Terrie C, Soulestin J, Gerault E, Feuilloley MGJ, et al. Active pseudo-multilayered films from polycaprolactone and starch based matrix for food-packaging applications. Eur Polym J. 2013;49:1234-42.

[2] Rhim JW, Park HM, Ha CS. Bio-nanocomposites for food packaging applications. Prog Polym Sci. 2013;38:1629-52.

[3] Luzi F, Fortunati E, Puglia D, Petrucci R, Kenny JM, Torre L. Study of disintegrability in compost and enzymatic degradation of PLA and PLA nanocomposites reinforced with cellulose nanocrystals extracted from Posidonia Oceanica. Polym Degrad Stab. 2015;121:105-15.

[4] Peelman N, Ragaert P, De Meulenaer B, Adons D, Peeters R, Cardon L, et al. Application of bioplastics for food packaging. Trends Food Sci Tech. 2013;32:128-41.

[5] Restuccia D, Spizzirri UG, Parisi OI, Cirillo G, Curcio M, Iemma F, et al. New EU regulation aspects and global market of active and intelligent packaging for food industry applications. Food Control. 2010;21:1425–35.

[6] Cushen M, Kerry J, Morris M, Cruz-Romero M, Cummins E. Nanotechnologies in the food industry – Recent developments, risks and regulation. Trends Food Sci Tech. 2012;24:30-46.

[7] Araújo A, Botelho G, Oliveira M, Machado AV. Influence of clay organic modifier on the thermal-stability of PLA based nanocomposites. Appl Clay Sci. 2014;88–89:144-50.

[8] Busolo MA, Fernandez P, Ocio MJ, Lagaron JM. Novel silver-based nanoclay as an antimicrobial in polylactic acid food packaging coatings. Food Addit Contam A. 2010;27:1617-26.

[9] Bodaghi H, Mostofi Y, Oromiehie A, Ghanbarzadeh B, Hagh ZG. Synthesis of clay–TiO_2 nanocomposite thin films with barrier and photocatalytic properties for food packaging application. J Appl Polym Sci. 2015;132:In press. doi: 10.1002/app.41764.

[10] Mihaly Cozmuta A, Peter A, Mihaly Cozmuta L, Nicula C, Crisan L, Baia L, et al. Active packaging system based on Ag/TiO_2 nanocomposite used for extending the shelf life of bread. Chemical and microbiological investigations. Packag Technol Sci. 2015;28:271-84.

[11] Pagno CH, Costa TMH, de Menezes EW, Benvenutti EV, Hertz PF, Matte CR, et al. Development of active biofilms of quinoa (*Chenopodium quinoa W.*) starch containing gold nanoparticles and evaluation of antimicrobial activity. Food Chem. 2015;173:755-62.

[12] Abou El-Nour KMM, Eftaiha Aa, Al-Warthan A, Ammar RAA. Synthesis and applications of silver nanoparticles. Arabian Journal of Chemistry. 2010;3:135-40.

[13] Echegoyen Y, Nerín C. Nanoparticle release from nano-silver antimicrobial food containers. Food Chem Toxicol. 2013;62:16-22.

[14] Kanmani P, Rhim JW. Physical, mechanical and antimicrobial properties of gelatin based active nanocomposite films containing AgNPs and nanoclay. Food Hydrocolloid. 2014;35:644-52.

[15] Emamifar A, Kadivar M, Shahedi M, Soleimanian-Zad S. Effect of nanocomposite packaging containing Ag and ZnO on inactivation of *Lactobacillus plantarum* in orange juice. Food Control. 2011;22:408-13.

[16] Fortunati E, Rinaldi S, Peltzer M, Bloise N, Visai L, Armentano I, et al. Nano-biocomposite films with modified cellulose nanocrystals and synthesized silver nanoparticles. Carbohydr Polym. 2014;101:1122-33.

[17] Artiaga G, Ramos K, Ramos L, Cámara C, Gómez-Gómez M. Migration and characterisation of nanosilver from food containers by AF4-ICP-MS. Food Chem. 2015;166:76-85.

[18] Lavorgna M, Attianese I, Buonocore GG, Conte A, Del Nobile MA, Tescione F, et al. MMT-supported Ag nanoparticles for chitosan nanocomposites: Structural properties and antibacterial activity. Carbohydr Polym. 2014;102:385-92.

[19] Valdes A, Mellinas AC, Ramos M, Burgos N, Jimenez A, Garrigos MC. Use of herbs, spices and their bioactive compounds in active food packaging. RSC Adv. 2015;5:40324-35.

[20] Ramos M, Jiménez A, Peltzer M, Garrigós MC. Characterization and antimicrobial activity studies of polypropylene films with carvacrol and thymol for active packaging. J Food Eng. 2012;109:513-9.

510 [21] Ramos M, Beltrán A, Peltzer M, Valente AJM, Garrigós MC. Release and antioxidant
511 activity of carvacrol and thymol from polypropylene active packaging films. LWT-Food Sci
512 Technol. 2014;58:470-7.
513 [22] Tawakkal ISMA, Cran MJ, Bigger SW. Effect of kenaf fibre loading and thymol
514 concentration on the mechanical and thermal properties of PLA/kenaf/thymol composites. Ind
515 Crop Prod. 2014;61:74-83.
516 [23] Ramos M, Fortunati E, Peltzer M, Dominici F, Jiménez A, Garrigós MC, et al. Influence of
517 thymol and silver nanoparticles on the degradation of poly(lactic acid) based nanocomposites:
518 Thermal and morphological properties. Polym Degrad Stab. 2014;108:158-65.
519 [24] Llorens A, Lloret E, Picouet PA, Trbojevich R, Fernandez A. Metallic-based micro and
520 nanocomposites in food contact materials and active food packaging. Trends Food Sci Tech.
521 2012;24:19-29.
522 [25] Tao F, Hill LE, Peng Y, Gomes CL. Synthesis and characterization of β-cyclodextrin
523 inclusion complexes of thymol and thyme oil for antimicrobial delivery applications. LWT-
524 Food Sci Technol. 2014;59:247-55.
525 [26] Chen H, Zhang Y, Zhong Q. Physical and antimicrobial properties of spray-dried zein-
526 casein nanocapsules with co-encapsulated eugenol and thymol. J Food Eng. 2015;144:93-102.
527 [27] Ezhilarasi PN, Karthik P, Chhanwal N, Anandharamakrishnan C. Nanoencapsulation
528 Techniques for Food Bioactive Components: A Review. Food Bioprocess Tech. 2013;6:628-47.
529 [28] Marques HMC. A review on cyclodextrin encapsulation of essential oils and volatiles.
530 Flavour and Fragrance Journal. 2010;25:313-26.
531 [29] Valdés A, Mellinas AC, Ramos M, Garrigós MC, Jiménez A. Natural additives and
532 agricultural wastes in biopolymer formulations for food packaging. Front Chem. 2014;2:1-10.
533 [30] Prosycevas I, Puiso J, Guobiene A, Tamulevicius S, Naujokaitis R. Investigation of Silver
534 Polymer Nanocomposites. Materials Science (MEDŽIAGOTYRA). 2007;13:188-92.
535 [31] Fortunati E, Armentano I, Iannoni A, Kenny JM. Development and thermal behaviour of
536 ternary PLA matrix composites. Polym Degrad Stab. 2010;95:2200-6.

[32] Ramos M, Jiménez A, Peltzer M, Garrigós MC. Development of novel nano-biocomposite antioxidant films based on poly (lactic acid) and thymol for active packaging. Food Chem. 2014;162:149-55.

[33] Gonçalves CMB, Tomé LC, Garcia H, Brandão L, Mendes AM, Marrucho IM. Effect of natural and synthetic antioxidants incorporation on the gas permeation properties of poly(lactic acid) films. J Food Eng. 2013;116:562-71.

[34] Wu Y, Qin Y, Yuan M, Li L, Chen H, Cao J, et al. Characterization of an antimicrobial poly(lactic acid) film prepared with poly(ε-caprolactone) and thymol for active packaging. Polym Adv Technol. 2014;25:948-54.

[35] Byun Y, Kim YT, Whiteside S. Characterization of an antioxidant polylactic acid (PLA) film prepared with α-tocopherol, BHT and polyethylene glycol using film cast extruder. J Food Eng. 2010;100:239-44.

[36] Hwang SW, Shim JK, Selke SEM, Soto-Valdez H, Matuana L, Rubino M, et al. Poly(L-lactic acid) with added α-tocopherol and resveratrol: optical, physical, thermal and mechanical properties. Polym Int. 2012;61:418-25.

[37] Rinaldi S, Fortunati E, Taddei M, Kenny JM, Armentano I, Latterini L. Integrated PLGA–Ag nanocomposite systems to control the degradation rate and antibacterial properties. J Appl Polym Sci. 2013;130:1185-93.

[38] Kanmani P, Rhim JW. Physicochemical properties of gelatin/silver nanoparticle antimicrobial composite films. Food Chem. 2014;148:162-9.

[39] Kumar R, Münstedt H. Silver ion release from antimicrobial polyamide/silver composites. Biomaterials. 2005;26:2081-8.

[40] Rhim JW, Wang LF, Hong SI. Preparation and characterization of agar/silver nanoparticles composite films with antimicrobial activity. Food Hydrocolloid. 2013;33:327-35.

[41] Jamshidian M, Tehrany EA, Imran M, Jacquot M, Desobry S. Poly-lactic acid: production, applications, nanocomposites, and release studies. Compr Rev Food Sci F. 2010;9:552-71.

[42] Raquez JM, Habibi Y, Murariu M, Dubois P. Polylactide (PLA)-based nanocomposites. Prog Polym Sci. 2013;38:1504-42.

565 [43] Rhim JW, Wang LF. Preparation and characterization of carrageenan-based nanocomposite
566 films reinforced with clay mineral and silver nanoparticles. Appl Clay Sci. 2014;97–98:174-81.
567 [44] Siracusa V, Rocculi P, Romani S, Rosa MD. Biodegradable polymers for food packaging:
568 a review. Trends Food Sci Tech. 2008;19:634-43.
569 [45] Sánchez-González L, Vargas M, González-Martínez C, Chiralt A, Cháfer M. Use of
570 essential oils in bioactive edible coatings: a review. Food Eng Rev. 2011;3:1-16.
571 [46] López-Mata M, Ruiz-Cruz S, Silva-Beltrán N, Ornelas-Paz J, Zamudio-Flores P, Burruel-
572 Ibarra S. Physicochemical, antimicrobial and antioxidant properties of chitosan films
573 incorporated with carvacrol. Molecules. 2013;18:13735-53.
574 [47] Samsudin H, Soto-Valdez H, Auras R. Poly(lactic acid) film incorporated with marigold
575 flower extract (*Tagetes erecta*) intended for fatty-food application. Food Control. 2014;46:55-
576 66.
577 [48] Fukushima K, Tabuani D, Arena M, Gennari M, Camino G. Effect of clay type and loading
578 on thermal, mechanical properties and biodegradation of poly(lactic acid) nanocomposites.
579 React Funct Polym. 2013;73:540-9.
580 [49] Gorrasi G, Pantani R. Effect of PLA grades and morphologies on hydrolytic degradation at
581 composting temperature: Assessment of structural modification and kinetic parameters. Polym
582 Degrad Stab. 2013;98:1006-14.
583 [50] Fortunati E, Armentano I, Iannoni A, Barbale M, Zaccheo S, Scavone M, et al. New
584 multifunctional poly(lactide acid) composites: Mechanical, antibacterial, and degradation
585 properties. J Appl Polym Sci. 2012;124:87-98.
586
587

588 **Figure Captions**

589 **Fig. 1.** DSC thermogram from the second heating scan (a), TG (b) and DTG (c) curves of PLA-
590 based films.

591 **Fig. 2.** FESEM surface images of PLA and active nanocomposite films.

592 **Fig. 3.** Visual observation of neat PLA and binary and ternary nanocomposite films.

593 **Fig. 4.** Visual appearance of neat PLA and active nanocomposite films at different testing days
594 under composting conditions at 58 °C.

595 **Fig. 5.** Disintegrability (%) of neat PLA and nanocomposite films at different times under
596 composting conditions at 58 °C (mean ± SD, n = 3). The line at 90 % represents the goal of
597 disintegrability test as required by the ISO 20200 standard. Different superscripts over different
598 samples at the same time indicate statistically significant different values ($p < 0.05$).

599

600 **Table 1.** PLA-based active nanocomposite films and thickness (mean ± SD, n = 3).

Formulation	PLA (wt%)	Ag (wt%)	Thymol (wt%)	Thickness (µm)
PLA	100	-	-	35 ± 4^{a}
PLA/Ag	99	1	-	39 ± 4^{a}
PLA/T6	94	-	6	40 ± 2^{a}
PLA/T8	92	-	8	41 ± 5^{a}
PLA/Ag/T6	93	1	6	42 ± 3^{a}
PLA/Ag/T8	91	1	8	39 ± 6^{a}

Different superscripts within the same column indicate statistically significant different values ($p < 0.05$).

601

Table 2. Characterization of neat PLA and nanocomposite films (mean ± SD, n = 3).

Formulation	T_g (ºC)	T_{ini} (ºC)	T_{max} (ºC)	WVP*10^{-14} (kg m s^{-1} m^{-2} Pa^{-1})	Reduction in WVP (%)	OTR*e (cm^3 mm m^{-2} day^{-1})
PLA	56.3 ± 2.2^a	320 ± 4^a	363 ± 2^a	1.84 ± 0.12^a	-	19.9 ± 2.1^a
PLA/Ag	53.7 ± 0.8^a	316 ± 4^a	354 ± 5^a	1.77 ± 0.01^a	4	26.2 ± 8.4^a
PLA/T6	43.3 ± 0.2^b	321 ± 3^a	351 ± 3^a	1.33 ± 0.11^b	27	18.5 ± 1.6^a
PLA/T8	43.5 ± 1.0^b	312 ± 2^a	354 ± 3^a	1.10 ± 0.09^c	40	20.7 ± 1.8^a
PLA/Ag/T6	42.6 ± 0.8^b	281 ± 3^b	332 ± 5^b	$1.12 \pm 0.05^{b,c}$	39	18.3 ± 1.1^a
PLA/Ag/T8	43.0 ± 0.4^b	284 ± 5^b	334 ± 6^b	$1.17 \pm 0.09^{b,c}$	36	18.3 ± 1.9^a

T_g: determined by DSC from the second heating scan at 10 ºC min^{-1}.
T_{ini} and T_{max}: determined by TGA at 10 ºC min^{-1} in N_2 atmosphere. Corresponding to the 2nd degradation step.
Different superscripts within the same column indicate statistically significant different values ($p < 0.05$).

602

603 **Table 3.** Optical properties of neat PLA and nanocomposite films (mean ± SD, n = 3).

	Colour parameters				Transparency
Formulation	*L**	*a**	*b**	*ΔE**	T_{500nm} (%)
PLA	47.36 ± 0.09^{a}	-0.19 ± 0.03^{a}	-0.12 ± 0.02^{a,c}	-	94.77 ± 0.01^{a}
PLA/Ag	46.67 ± 0.29^{b}	1.53 ± 0.03^{b}	8.04 ± 0.07^{b}	8.37 ± 0.09^{a}	91.31 ± 0.01^{b}
PLA/T6	48.25 ± 0.20^{c}	-0.15 ± 0.02^{a}	-0.22 ± 0.04^{c}	0.89 ± 0.16^{b}	93.53 ± 0.03^{c}
PLA/T8	48.33 ± 0.31^{c}	-0.28 ± 0.02^{c}	-0.06 ± 0.02^{a}	0.97 ± 0.34^{b}	94.41 ± 0.03^{d}
PLA/Ag/T6	45.47 ± 0.27^{d}	1.21 ± 0.03^{d}	8.83 ± 0.08^{d}	9.25 ± 0.10^{c}	90.21 ± 0.01^{e}
PLA/Ag/T8	46.38 ± 0.22^{b}	1.04 ± 0.02^{e}	9.57 ± 0.06^{e}	9.81 ± 0.06^{d}	90.80 ± 0.02^{f}

Different superscripts within the same column indicate statistically significant different values ($p < 0.05$).

604

(a)

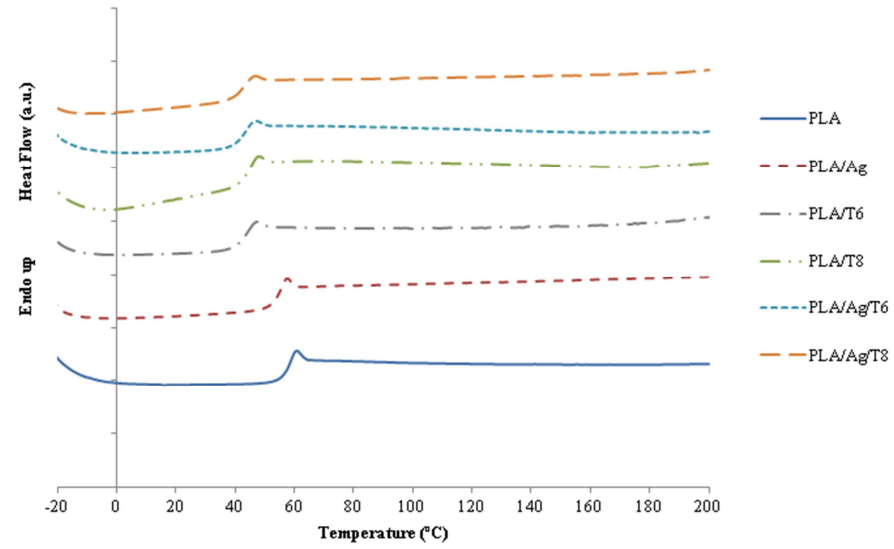
Heat Flow (a.u.)
Endo up
-20
0
20
40
60
80
100
120
140
160
180
200
Temperature (°C)
PLA
PLA/Ag
PLA/T6
PLA/T8
PLA/Ag/T6
PLA/Ag/T8

(b)

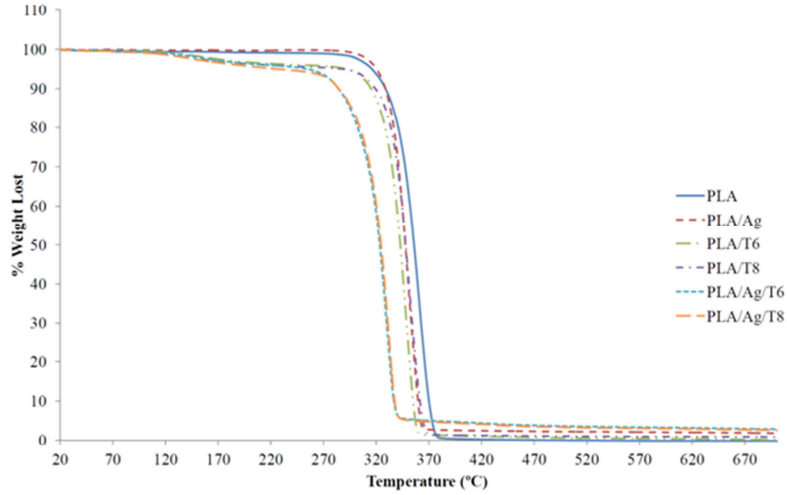
% Weight Lost
110
100
90
80
70
60
50
40
30
20
10
0
20
70
120
170
220
270
320
370
420
470
520
570
620
670
Temperature (°C)
PLA
PLA/Ag
PLA/T6
PLA/T8
PLA/Ag/T6
PLA/Ag/T8

(c)

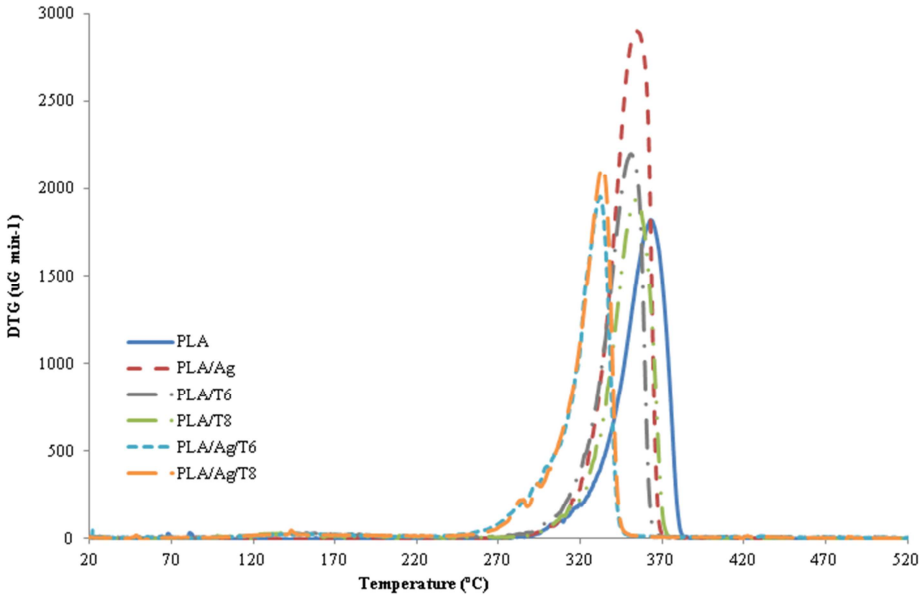
DTG (uG min-1)
3000
2500
2000
1500
1000
500
0
20
70
120
170
220
270
320
370
420
470
520
Temperature (°C)
PLA
PLA/Ag
PLA/T6
PLA/T8
PLA/Ag/T6
PLA/Ag/T8

Figure 2

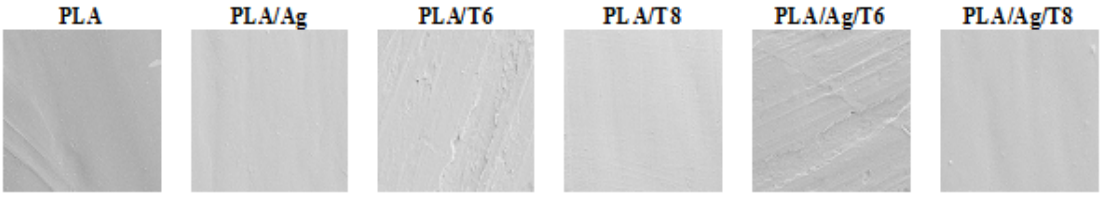

10 um Mag. 2.0 KX

Figure 3

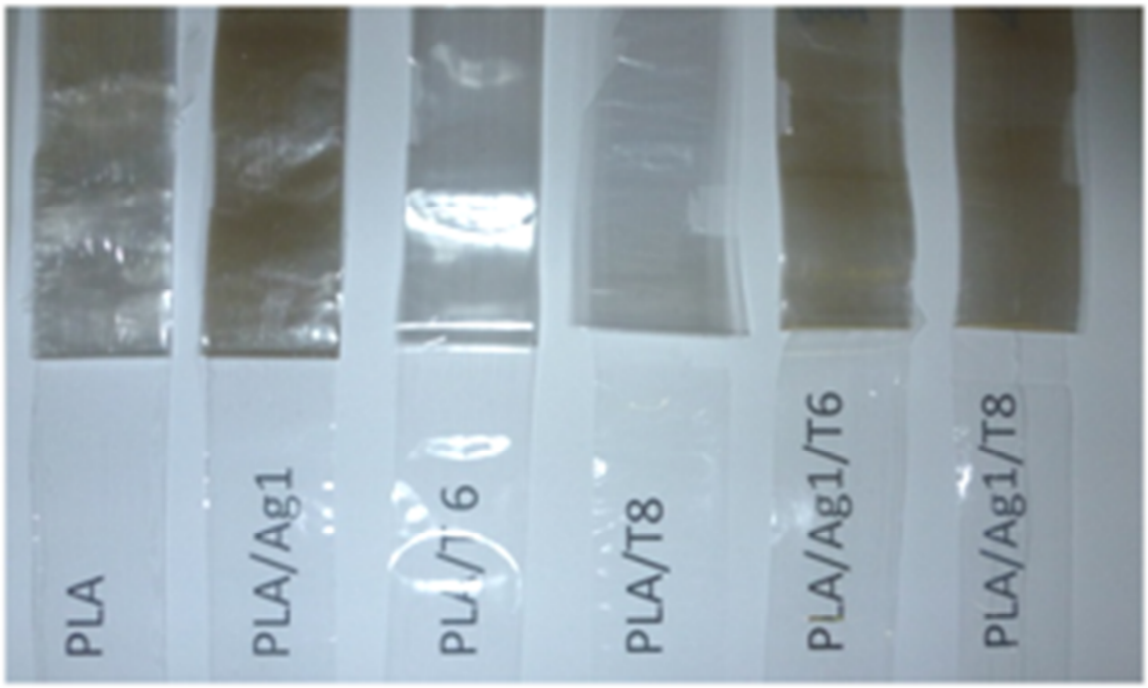

Figure 4

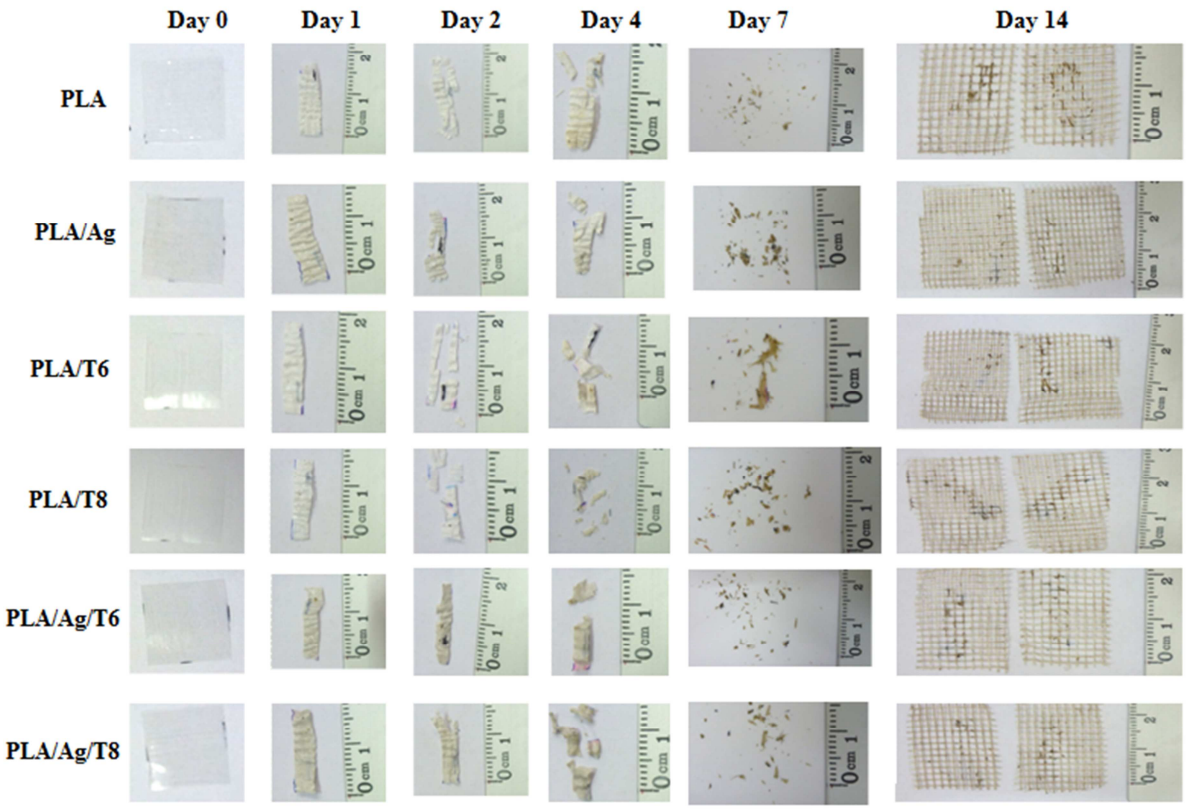

Figure 5